

## Fiber orientation measurement using polarization imaging

N. LECHOCINSKI and S. BREUGNOT, *Bossa Nova Technologies*,  
606 Venice Blvd, Suite B, Venice, CA 90291.

### Synopsis

In this paper, we present a new technique to determine the orientation of hair fiber, a key parameter in the evaluation of visual appearance of hair. Using polarization imaging and image analysis tools, we are able to measure the orientation of hair fiber for each pixel in the image. A theoretical analysis of the optical set-up is presented. Experimental data on a single fiber, hair tress, and complete head are given. Application to shampoo and conditioner is also demonstrated.

### INTRODUCTION

Visual appearance of hair is defined by multiple parameters: color, shine (external reflection), and chroma (internal reflection). Another important parameter is the orientation of the hair fiber. Different methods have been presented to measure fiber orientation. These methods are using conventional imaging followed by image processing, which analyzes the texture in order to deduct the orientation of the fiber (1–3). Automatic measurement of the orientation of the hair fiber can be a difficult task as the image processing techniques are strongly affected by parameters such as the quality of the illumination and the color of the fiber.

In this paper, we propose a new technique to measure the orientation of hair fiber. Based on polarization analysis, this technique allows the measurement of a physical parameter directly connected to the orientation of the fiber for each pixel of the image. This technique operates for every kind of hair, dark to blond, straight to curly.

### SCIENTIFIC BACKGROUND

#### BIREFRINGENCE OF HAIR FIBER

Birefringence is the decomposition of a ray of light into two rays (the ordinary ray and the extraordinary ray) when it passes through certain types of material, depending on the polarization of the light. This effect can occur only if the structure of the material is anisotropic (directionally dependent). If the material has a single axis of anisotropy, birefringence can be formalized by assigning two different refractive indices to the material for different polarizations. The birefringence magnitude is then defined by  $\Delta n = n_e - n_o$ ,

where  $n_e$  and  $n_o$  are the refractive indices for polarization parallel (extraordinary) and perpendicular (ordinary) to the axis of anisotropy respectively. The retardance  $R$  of the birefringent material is given by  $R = 2\pi/\lambda \Delta n d$ , where  $d$  is the thickness of the material and  $\lambda$  the wavelength of the light.  $R = \pi$  (or 180 degree) corresponds to a half-wave plate ( $\Delta n d = \lambda/2$ ) and  $R = \pi/2$  (or 90 degree) to a quarter-wave plate ( $\Delta n d = \lambda/4$ ).

Hair fiber exhibits a birefringence in the visible and near-infrared spectrum. Numerous papers have been published about the measurement of the birefringence of hair using different methods (4). The birefringence of hair fiber is mainly due to the geometry of the cortical region of the human hair, which also gives hair its elasticity properties. Typical birefringence values are  $\Delta n = 1-0.5\%$ . The birefringence axis is parallel and perpendicular to the fiber axis (Figure 1). The analysis of the birefringence of hair can also lead to the identification of hair defects (5).

#### INTERACTION OF POLARIZED LIGHT WITH HAIR FIBERS

Hair has a very specific visual appearance. Hair fibers can be considered as transparent and partially absorptive fibers with small steps at their surface (hair cuticle). This structure causes the visual appearance of hair fiber. It is widely accepted that hair visual appearance comes from three different interactions of light with the hair fibers resulting in three components of light (Figure 2):

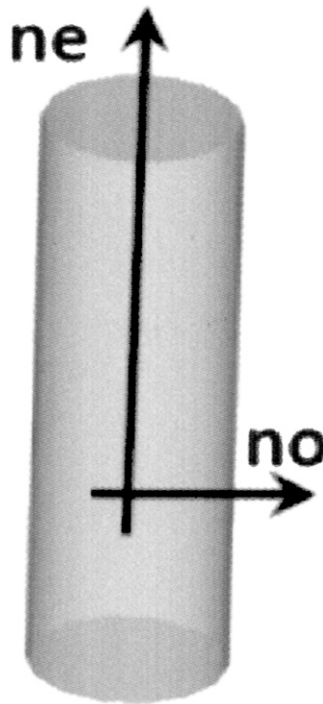


Figure 1. Birefringence axis of hair fiber.

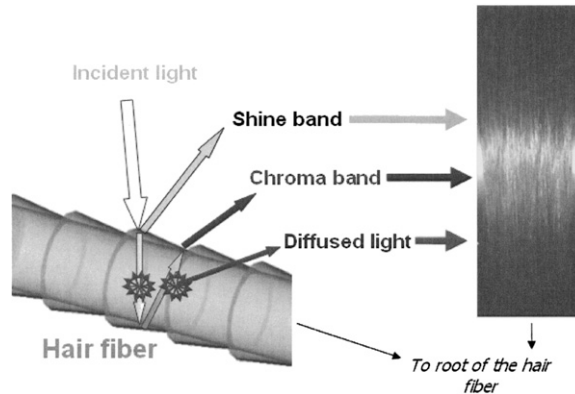


Figure 2. Interactions of light with hair fiber (left). Illustration on a hair tress placed on a curved surface (right).

- The first component is called the shine. It is caused by the reflection of the light on the surface of the hair fiber. Since this component consists of an external reflection, it remains polarized (in case of a polarized illumination) and it is “white” (more precisely of the same color as the illuminating light).
- The second component is called the chroma. It is caused by the refraction of the incident light in the hair fiber and the reflection on the back surface. Since this component only experiences reflections and refractions, it remains polarized (in case of a polarized illumination). Since the light travels through the hair fiber, the chroma is colored.
- The last component is called the diffused light. It is caused by the light is refracted into the hair fiber and scattered by pigments inside the hair fiber. Since this component experiences diffusion, it is depolarized (in case of a polarized illumination). Since the light travels through the hair fiber, it is colored.

To measure the orientation of the hair fiber, we will focus on the chroma reflection, which carries the birefringence information as the light is transmitted through the fiber and back-reflected. We can then simply describe the interaction of polarized light with hair fiber using a simple model where the hair fiber is locally a birefringent material of birefringence  $\Delta n$  (Figure 3) with its axis at an angle  $\theta$  with the vertical axis.

If we illuminate the hair fiber with a polarized light, we detect three components of the backscattered light:

- Shine: Same polarization as the incident light
- Chroma: Polarized light but different polarization due to the birefringence
- Diffuse: Un-polarized light

#### MEASUREMENT OF THE ORIENTATION OF HAIR FIBER

In order to measure the orientation of the hair fiber, we need to detect the influence of the chroma and the axis of the birefringence. A simple optical set-up to measure the orientation of the axis of a *birefringent* material in a transmission mode is to illuminate and detect with parallel polarization (Figure 4).

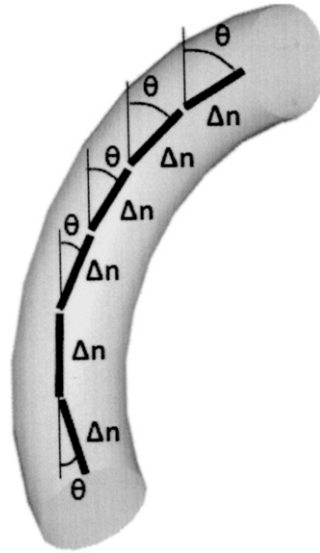


Figure 3. Simple model: Hair fiber = birefringent material.

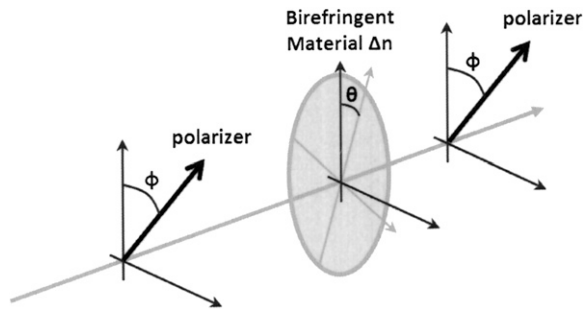


Figure 4. Birefringence axis measurement set-up (transmission).

A simultaneous rotation of both polarizers (Angle  $\phi$  compared to vertical axis) allows the collection of the transmitted light intensity versus the orientation of the polarizer  $\phi$ . The transmitted light intensity  $I$  is given by the following formula:

$$I(\phi, \theta) = \frac{1}{4} \left\{ 1 + \frac{1}{2} (1 + \cos(R)) + \frac{1}{2} (1 - \cos(R)) \cos[4(\theta - \phi)] \right\}$$

Figure 5 shows the transmitted light intensity versus the orientation  $\phi$  of the polarizer for various orientations of angle  $\theta$ .

We observe a sinusoidal signal where the amplitude does not depend on the orientation of the birefringence axis  $\theta$  but where the phase of the signal is related to  $\theta$ . We can also observe that there is a 90 degree uncertainty as a vertical birefringent material delivers the same signal as a horizontal one.

For hair fiber, we proceed to a similar set-up, except that we are working in a reflection mode (Figure 6).

The intensity of light backscattered by the hair fiber is composed of three components:

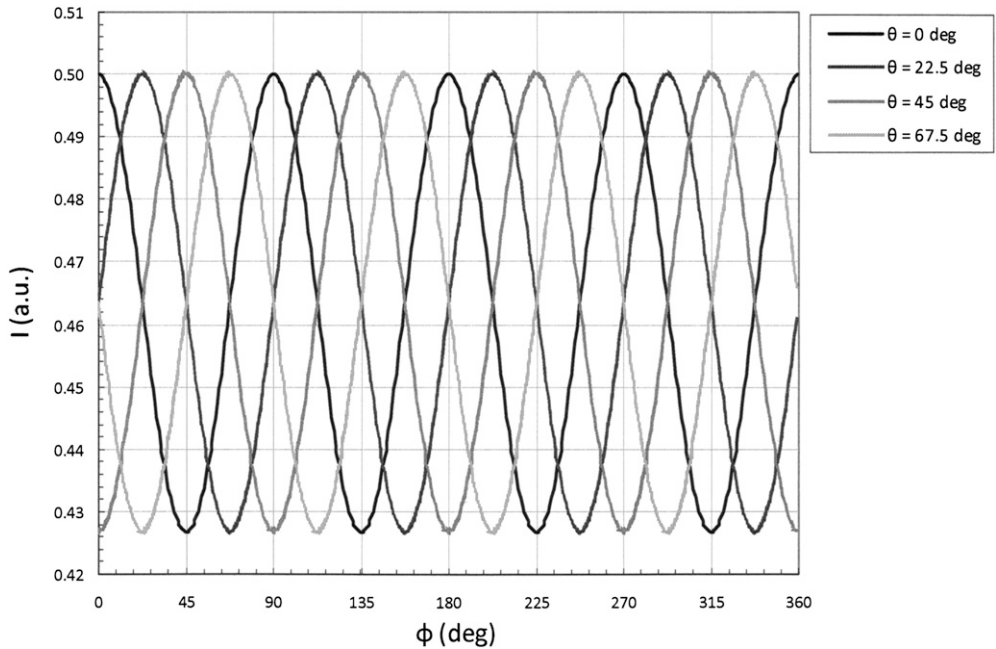


Figure 5. Transmitted light intensity versus the orientation  $\phi$  of the polarizer for various orientations of angle  $\theta$ .

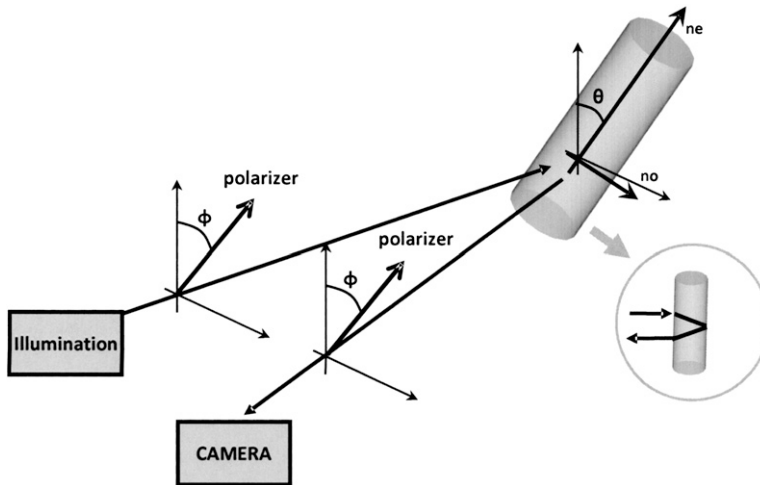


Figure 6. Set-up.

- $I_s$  (Shine, constant with  $\phi$ )
- $I_c(\phi, \theta)$  (Chroma, varies with  $\phi$  and  $\theta$ )
- $I_d$  (Diffuse, constant with  $\phi$ )

Compared to the case of a birefringent material in the transmission mode, we now have a larger continuous level due to the diffuse and shine light, with the modulation due to the chroma. The retardance for a single hair fiber in reflection mode is  $R = 2\pi/\lambda \Delta n 2d$ . With

$d = 70 \mu\text{m}$ ,  $\lambda = 0.83 \mu\text{m}$ , and  $\Delta n = 0.5\%$ , we can estimate  $R = 5.3 \text{ rad}$  ( $56^\circ$ ). Measuring the phase of the sinusoidal signal will allow the measurement of the angle of orientation  $\theta$  of the hair fiber.

## PRESENTATION OF THE SET-UP

### SPECTRAL BAND SELECTION

In order to have a system working on every type of hair (from dark to light), a selection of the best spectral band where the system will be operating needs to be done. To access the birefringence measurement and the chroma reflection, we have to use a spectral band where every type of hair is transparent. Figure 7 shows the total attenuation coefficient for different kind of hair versus the wavelength (6).

Above 800 nm, the total attenuation coefficient becomes acceptable. In the near-infrared region (NIR), we can use silicon camera, dichroic polarizers and NIR led for the illumination. Figure 8 shows the comparison of the picture taken the visible and near-infrared region for a variety of hair tresses with different shades.

### EXPERIMENTAL SET-UP

The set-up (Figure 9) is composed of a camera, a ring of NIR LEDs (operating in pulse mode) and a NIR polarizer mounted on a rotation stage. The camera is connected to a computer for the acquisition of the images, the signal processing and data visualization. As the NIR polarizer rotates, it triggers the flash of the NIR polarized illumination and successive polarization images are acquired. Automatic signal processing analyzes the sinusoidal variation for each pixel of the image and calculates the corresponding angle of orientation. The acquisition of the polarization images takes about 1 second, followed by

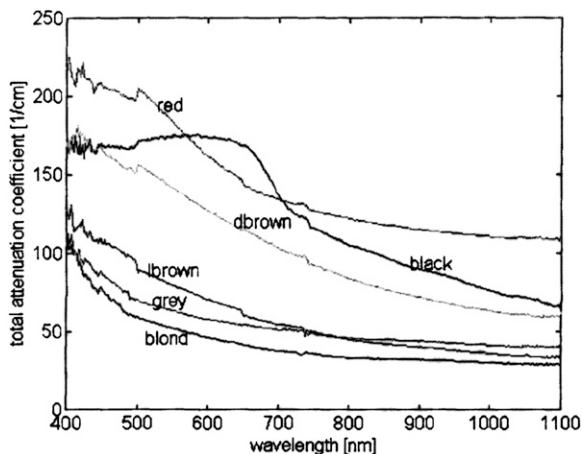
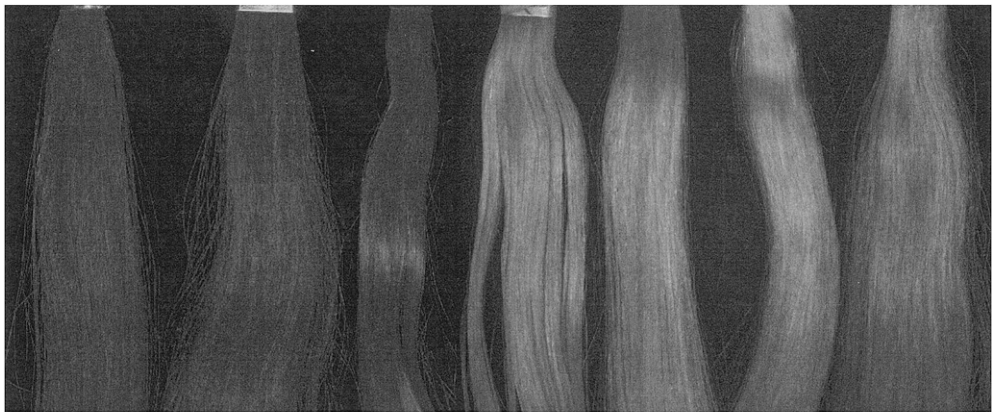


Figure 7. Total attenuation coefficient for different kinds of hair versus the wavelength (from visible to near-infrared).



(a)



(b)

**Figure 8.** (a) Intensity images in the visible spectrum for tresses of various shades (from left to right: black, dark brown, medium brown, dark brown with red dye, blond, bleached, grey 10%–90%). (b) Corresponding images in the NIR region.

the image processing (~5–10s). The orientation image is then visualized. Different tools allow statistical analysis in regions of interest (ROI) in the image.

The resolution of our imaging system permits to discriminate a single hair fiber, i.e. one pixel corresponds to approximately 80–100 micron on the hair fiber plane. This will allow our simple model to be valid.

#### EXPERIMENTAL VALIDATION OF THE CONCEPT

We proceed to two basic experiments to validate the concept of the measurement:

- Birefringence measurement (extraction of the sinusoidal signal over a region of interest and measurement of the angle of orientation)
- Evaluation of the angle measurement precision

BIREFRINGENCE MEASUREMENT

We are using two hair tresses (blond and dark). Figure 10 shows the intensity  $I$  (a.u.) versus the angle of the polarizer  $\phi$ , in a region of interest where the orientation of the hair is constant, for three orientations of the hair tress ( $\theta = -10^\circ, 0^\circ$ , and  $10^\circ$ ).

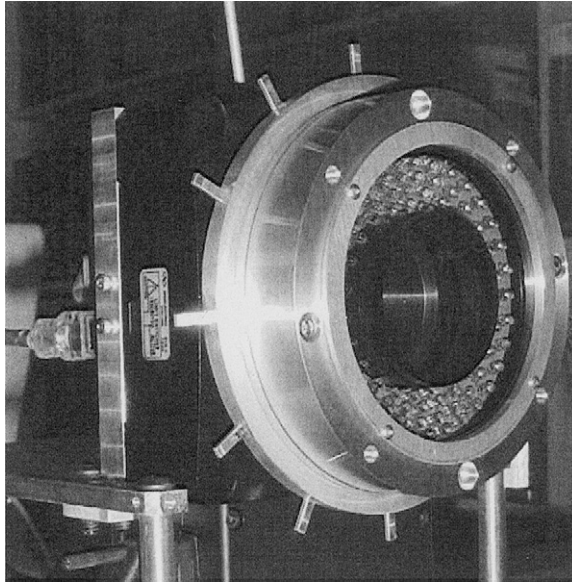


Figure 9. Photo of set-up.

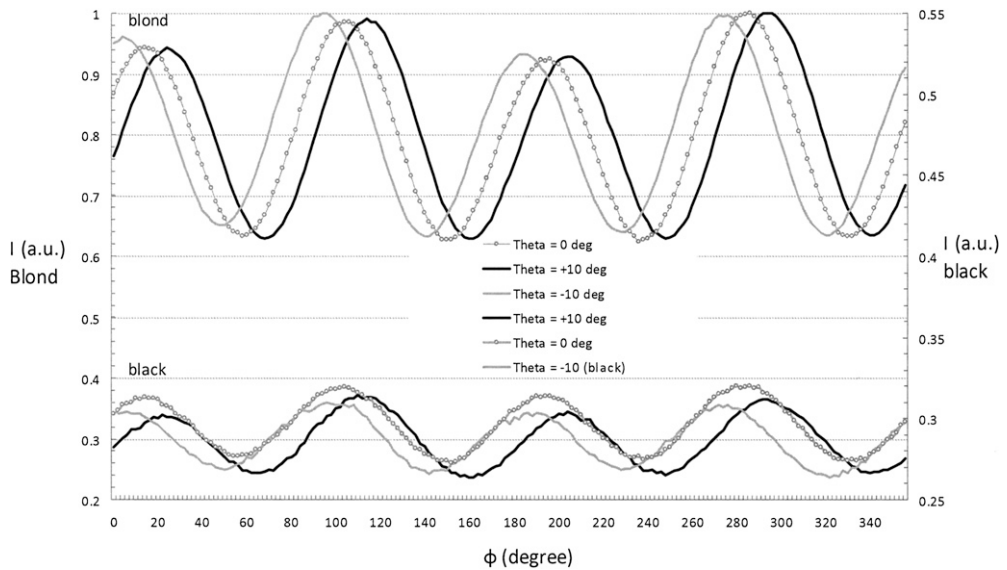


Figure 10. Signal versus the angle of the polarizer  $\phi$ .



As expected by the theory, we observe a sinusoidal signal for both hair tresses. It is easy to observe the  $\pm 10^\circ$  phase shift of the signal due to the orientation of the hair tress, on both hair types. The average intensity and its modulation for dark hair is about 3 times less than the blond hair. We can observe the measurement noise on the dark hair signal. From this data, we can easily measure the angle of orientation  $\theta$ .

#### ANGLE PRECISION

In order to measure the angle of orientation  $\theta$  and the precision of the measurement, we place a straightened blond hair bundle on a precision mechanical rotation stage (Figure 11).

We measure the angle of orientation  $\theta$  versus the theoretical angle  $\theta$  in order to evaluate the precision of the angle measurement. Figure 12 shows the measured angle  $\theta$  versus the theoretical angle  $\theta$ .

The experimental data are in very good agreement with the theory. Figure 13 shows the measured angle  $\theta$  versus the theoretical angle  $\theta$  for a small variation of  $\theta$ .

We estimate the angle precision to be  $\pm 0.1^\circ$ . This is precise enough for the type of experiment and image we will carry on.

## EXPERIMENTAL RESULTS

#### STUDY OF FLYAWAY HAIR

Single hair fiber resolution is achieved at a given stand-off distance by selecting the appropriate resolution and objective lens for the camera. Fig 14 shows the image of a single hair

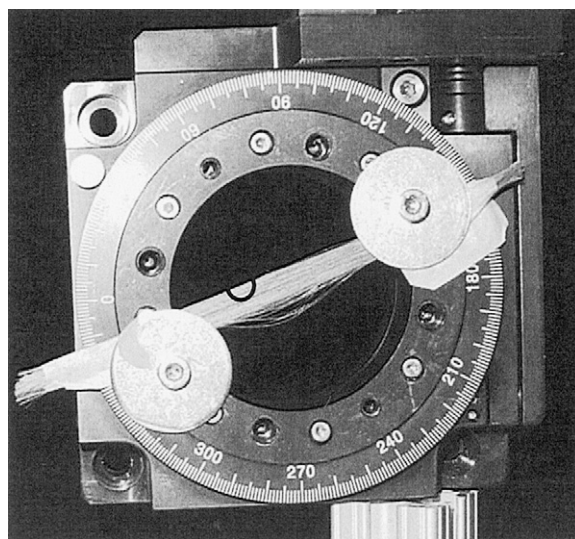


Figure 11. Blond hair bundle on a precision mechanical rotation stage.

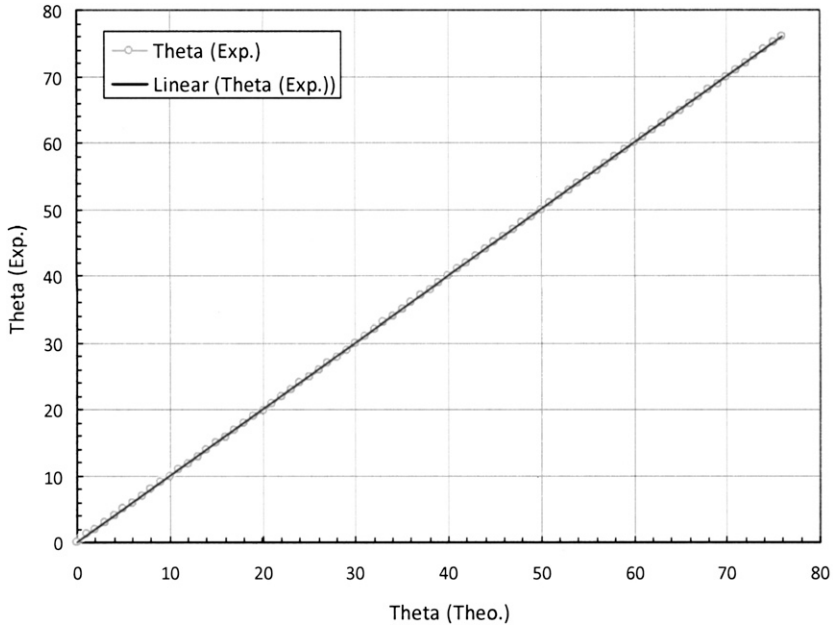


Figure 12. Measured angle  $\theta$  versus the theoretical angle  $\theta$ .

fiber (blond) in the NIR (a) and its corresponding orientation image (b) In those images, the pixel resolution is about  $80 \mu\text{m} \times 80 \mu\text{m}$ . We can detect without any problem the orientation of the single hair fiber. An application of single hair fiber imaging is the detection and identification of flyaway hair. Flyaway hair is caused when hair strands pick up

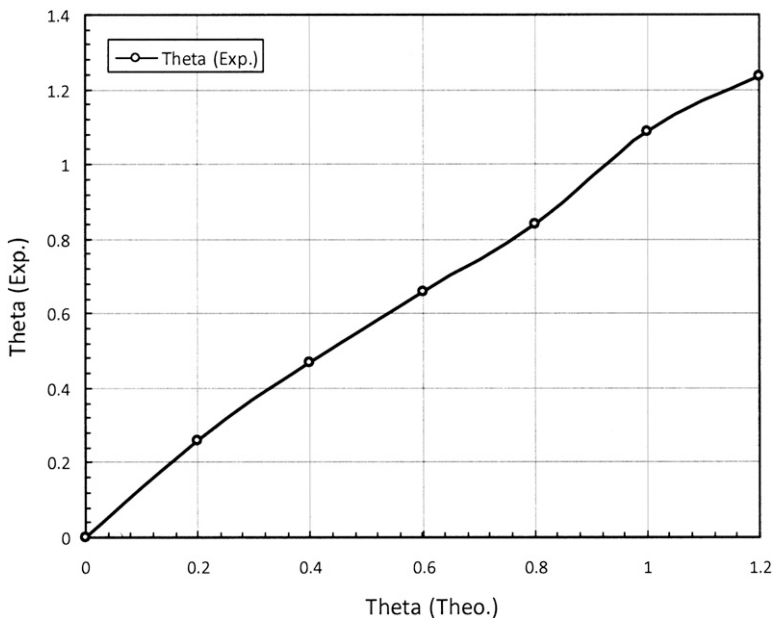


Figure 13. Measured angle  $\theta$  versus the theoretical angle  $\theta$  for a small variation of  $\theta$ .

positive charges and begin to repel from the rest of hair. Figure 15 shows the intensity image of three bleached hair tress (a) and their corresponding orientation measurements (b).

The computation of the angular distributions in the selected regions of interest (ROI) permits to quantify the flyaway as shown in Figure 16.

Subtracting the histogram of the ROI2 to the histogram of the ROI1 gives the angular distribution of the flyaway. The distribution is mostly homogeneous across the range of angles, which is translated by an offset of the histogram in the ROI2 compared to the ROI1. However, the distribution of the flyaway shows a little bump around 10–15 deg, which shows that the flyaway has a greater tendency to repel from the rest of the hair tress at this orientation in the environmental conditions of the measurement. Single fiber resolution measurement with this technique not only permits to easily detect flyaway hair, but also to add information by giving the orientation of the flyaway relatively to the rest of the hair tress.

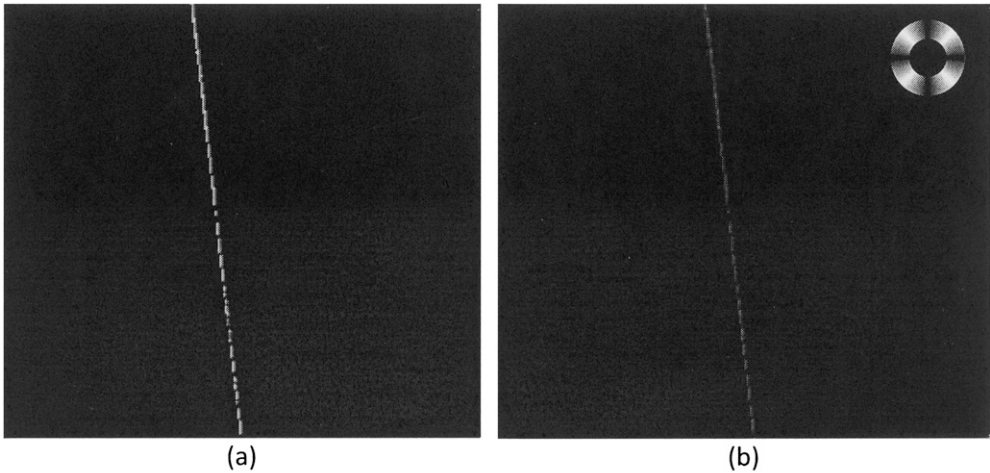


Figure 14. Image of a single hair fiber in the NIR (a) and its corresponding orientation image (b).

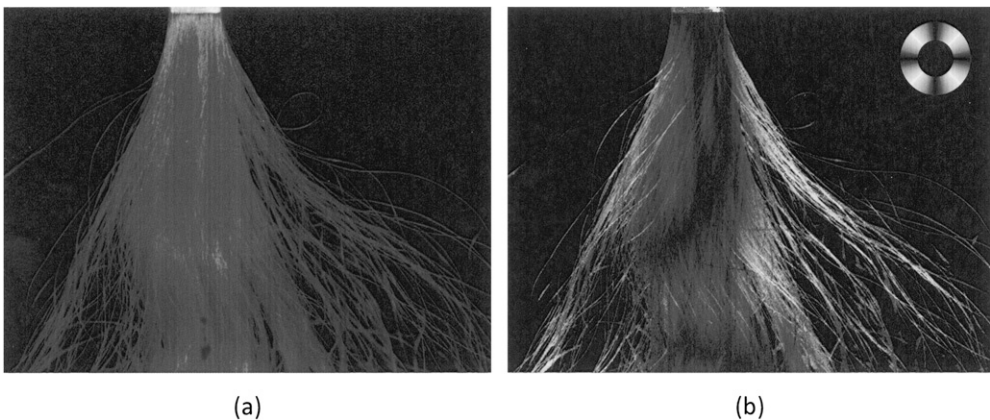


Figure 15. Intensity image of three bleached hair tresses (a) and their corresponding orientation measurement (b).

MEASUREMENT OF DEGREE OF CURL AND STYLE LONGEVITY

In Figure 17 below, three bleached hair tresses with different degrees of curl are imaged (a) intensity and (b) orientation.

The computation of the histogram (Figure 18) for each hair tress shows different patterns according to the degree of curl. As a matter of fact, as the degree of curl increases (from tress 1 to tress 3), the angular distribution becomes wider (standard deviation increases).

The computation of the standard deviation of the histograms (parameter  $W$ ) shows that the higher the degree of curl is, the greater the  $W$  is, as shown in Table I. The angular distribution widens as the degree of curl increases to eventually tend towards a flat distribution for a very high degree of curl.

Such analysis can allow the evaluation of the style longevity under high humidity conditions for example or allow the classification of tresses according to their degree of curl.

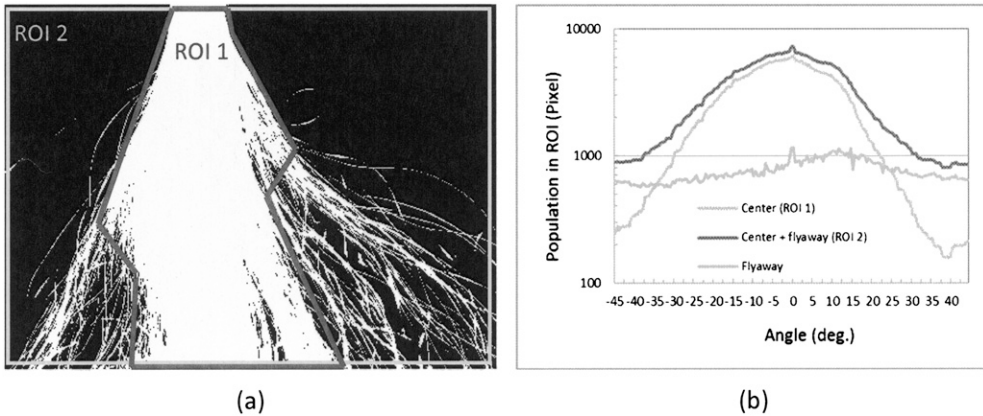


Figure 16. (a) Selection of two regions of interest for the center part of the hair tress (ROI 1) and the complete image (ROI2), histograms in the respective ROIs (b).

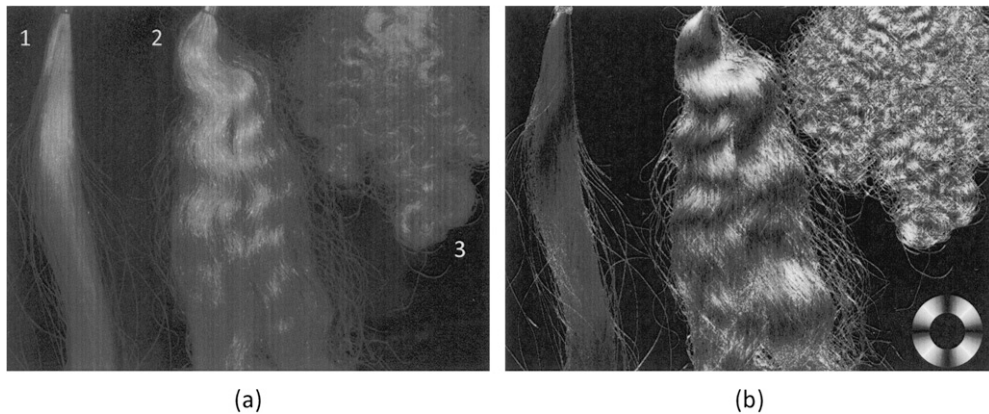


Figure 17. Intensity image of three bleached hair tresses (a) and the corresponding orientation (b).

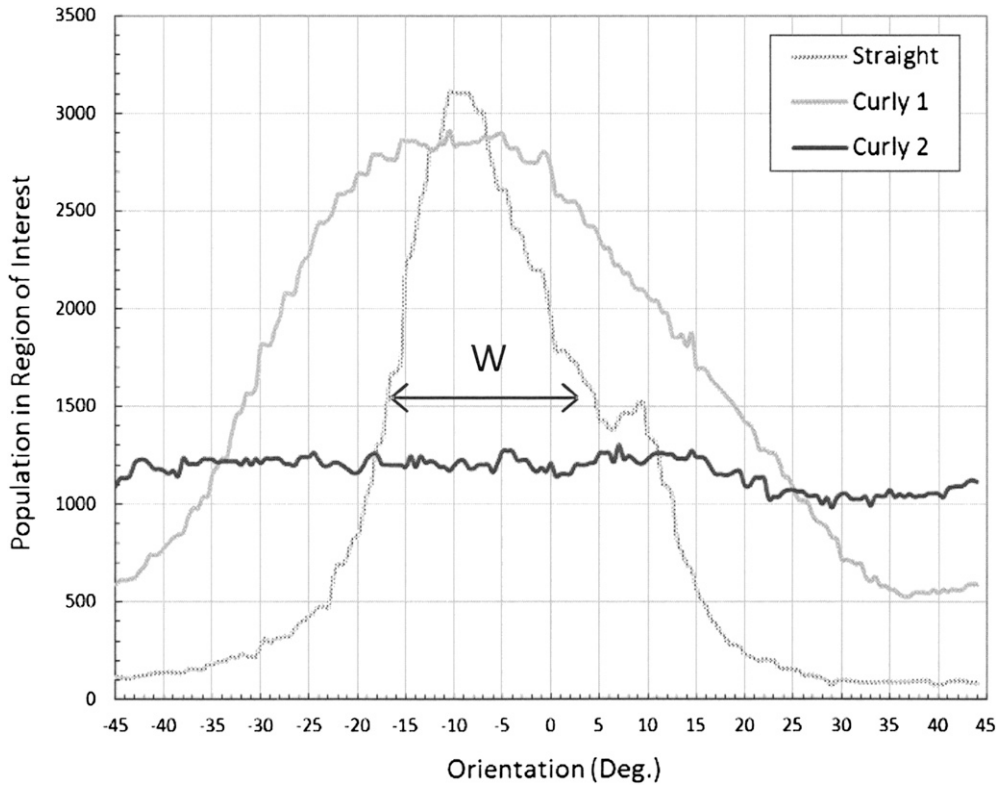


Figure 18. Histograms representing the angular distribution for each tress.

SHAMPOO AND CONDITIONER MEASUREMENTS ON HAIR TRESSES

Using vertically hung tresses of any shade, it is possible to measure the efficacy of a treatment such as shampoo and conditioner on the alignment of the hair fibers. Figure 19 below shows images in the NIR region of two vertically hung oriental hair tresses (blond and brown). Images on the left show the untreated hair tresses while the images on the right show the hair tresses after application of a shampoo + conditioner that claims to smooth the hair and facilitate the combing.

The hair appears more aligned in the orientation images (Figure 19 (b)) as the proportion of fibers with a small angle relatively to the vertical (black pixels) is increased.

Table I  
Table of Mean Values and Standard Deviations (W) of the Histograms

	Mean (deg)	W (deg)
Straight	-4.8	13.2
Curly 1	-4.7	19.9
Curly 2	n/a	∞

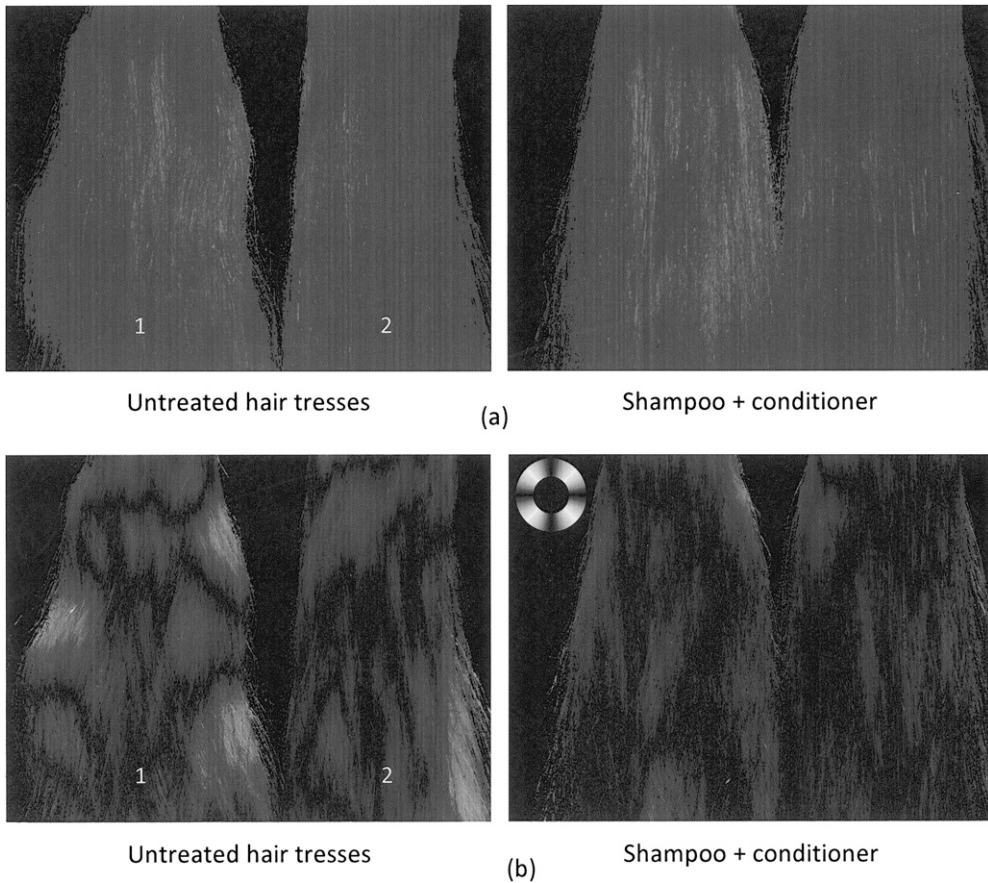


**Figure 19.** (a) NIR images of vertically untreated oriental hair tresses (left) and the same tresses with a shampoo + conditioner treatment (right) and their corresponding orientation images (b).

Table II shows the calculation of the standard deviations for each tress. The results show a decrease of the standard deviation of about 33% on both tresses after application of the shampoo and conditioner. The hair is about three times *more aligned* after treatment.

#### FULL HEAD

*In vivo.* The system resolution and field of view coupled with a small acquisition time (about 1s) allows *in vivo* measurements on human models. Figure 20 shows two examples of measurement for two different shades of hair.

**Table II**

Table Showing the Standard Deviation Variations of the Histograms for Untreated and Treated Hair Tresses

	W (deg.) tress 1	W (deg.) tress 2
Untreated	$7.9 \pm 0.2$	$6.5 \pm 0.3$
Shampoo + conditioner	$5.3 \pm 0.1$	$4.4 \pm 0.1$
Variation (%)	-33	-32



Figure 20. Example of two *in vivo* measurements on human heads for two different shades of hair.

The same applications presented before can be applied to *in vivo* measurements thanks to its fast acquisition time. No blur has been observed in the image.

## CONCLUSION

We have presented a new method to measure the angle of orientation of hair fiber, based on polarization analysis and imaging. Contrary to current methods that use conventional imaging followed by image processing, our technique delivers the measurement of the

orientation of the birefringence axis of the hair fiber, for each pixel of the image. The measurement operates on single fiber, hair trees, and full head, for laboratory and in-vivo applications. Thanks to near-infrared illumination, every type of hair can be analyzed, from blond to dark, straight to curly. Application for shampoo/conditioner evaluation is demonstrated. In-vivo measurement on real model can also be done as the image acquisition is fast enough as it takes about one second. This technique permits to study precisely the influence of the orientation of hair fiber on the visual appearance. It opens numerous potential applications for product development, product evaluation and claim substantiation. This new sensor opens the door to the definition of new measurement procedures and new parameters in order to fully quantify the visual appearance of hair. This technique has been patented (Patent pending: application US12/567,579).

## REFERENCES

- (1) S. Hariharan, S. A. Sathyakumar, and P. Ganesan, Measuring of fibre orientation in nonwovens using image processing, [www.fibretofashion.com](http://www.fibretofashion.com)
- (2) Y. J. Han, Y. J. Cho, W. E. Lambert, and C. K., Identification and measurement of convolutions in cotton fiber using image analysis, *Artificial Intelligence Review*, 12(1-3), 201-211 (1998).
- (3) K. E. Duckett and C. C. Cheng, The detection of cotton fiber convolutions by the reflection of light, *Textile Res. J.* 42, 263-268 (1972).
- (4) R. K. Curtis and D. R. Tyson, Birefringence: Polarization microscopy as a quantitative technique of human hair analysis, *J. Soc. Cosmet. Chem.*, 27, 411-431 (1976).
- (5) A. C. Brown, R. B. Belser, R. G. Crouse, and R. F. Wehr, A congenital hair defect: Trichoschisis with alternating birefringence and low sulfur content, *J. Invest. Dermatol.*, 54, 496-509 (1970).
- (6) Tjitske van Kampen, Optical properties of hair, Masters project, January 1, 1997.